

Step-graded buffer layer study of the strain relaxation by transmission electron microscopy

D. González^a, D. Araújo^a, S.I. Molina^a, A. Sacedón^b, E. Calleja^b, R. García^a

^a*Departamento de Ciencia de los Materiales e IM y QI, Universidad de Cádiz, Apartado 40, 11510 Puerto Real (Cádiz), Spain*

^b*Departamento de Ingeniería Electrónica, Escuela Técnica Superior de Ingeniería de Telecomunicación, Universidad Politécnica de Madrid, Ciudad Universitaria, 28040 Madrid, Spain*

Abstract

The lattice relaxation behavior in an $\text{In}_x\text{Ga}_{1-x}\text{As}/\text{GaAs}$ linearly step-graded structure is studied by transmission electron microscopy (TEM). From the misfit dislocation densities measured by TEM at each interface the relaxation parameters such as strain and percentage relaxation are deduced for each layer. The obtained results are compared with the predictions of the Dunstan et al. model which describe the dislocation behavior during relaxation in such structures. A different relaxation behavior than that described by Dunstan et al. is observed. This is attributed to the fact that the individual layer thickness is lower than the critical layer thickness of Dunstan et al. Work-hardening processes are found to induce a linear increase in the residual strain with increasing layer thickness.

Keywords: Transmission electron microscopy; Semiconductors; Gallium arsenide; Relaxation phenomena

1. Introduction

The modern optoelectronics and microelectronics technologies require materials having efficient optoelectronic properties (carrier mobility, relaxation lifetimes etc.) and a photon emission in the range of the minimum absorption of light guides (1.51 and 1.36 eV). Therefore, during the last few years, many optoelectronics devices have been based upon $\text{In}_x\text{Ga}_{1-x}\text{As}/\text{GaAs}$ heterostructures. The advantage and/or disadvantage of this system is the lattice mismatch between the $\text{In}_x\text{Ga}_{1-x}\text{As}$ and the GaAs layers. This lattice mismatch permits growth of strained layers that can increase laser efficiency but, if the layer thickness exceeds the critical thickness, the relaxation induces defects that can degrade the optoelectronic properties of the device.

When variations in the In concentration in $\text{In}_x\text{Ga}_{1-x}\text{As}$ alloys are less than 18 at.% In, threading dislocations are absent in the epitaxial layer and dislocations propagate from the heterointerface into the GaAs material while, for variations greater than 18 at.% In, dislocations appear to propagate into both the substrate and the epilayer [1]. To prevent such defect formation, buffer layers are grown between the

GaAs substrate and the $\text{In}_x\text{Ga}_{1-x}\text{As}$ layers to adapt the lattice parameter. Various solutions have been recently proposed. Among them, graded buffer layers [2-4], step-graded buffer layers [5] and multilayers and superlattices [6, 7] seem to be the most efficient systems to filter dislocations. Up to now, it is not clear which of these buffer layer structures is the most efficient in obtaining relaxed defect free layers. However, one of the important advantages of step-graded buffers is the possibility of probing the relaxation layer by layer. Indeed, the misfit and the residual strain can be analyzed for each layer of the stack.

In this study, relaxation in a step-graded buffer is studied by high resolution transmission electron microscopy (HREM), cross-sectional transmission electron microscopy (XTEM) and planar-view transmission electron microscopy (PVTEM). From the misfit dislocation (MD) distribution at each interface, the percentage relaxation, effective misfit and residual strain are deduced for each layer. The residual strain at the top layer is also deduced by double-crystal X-ray diffraction and by photoluminescence. The obtained values are used as a reference to compare with the TEM data. Following these measurements, an empirical model of strain relaxation in step-graded layers is

proposed. Finally, from PVTEM observations, a dislocation density lower than 10^5 cm^{-2} is measured at the top layer. This demonstrates the potential possibilities of such buffer layer that can reach a structural quality in the range of commercial substrates.

2. Experimental technique

An $\text{In}_x\text{Ga}_{1-x}\text{As}$ step-graded layer structure grown on a GaAs(001) substrate is analyzed. Fig. 1 displays the sample structure that consists of six $\text{In}_x\text{Ga}_{1-x}\text{As}$ layers 125 nm thick. The layer steps of concentration are 5, 10, 15, 20, 25 and 30 at.%. A top layer of $\text{In}_x\text{Ga}_{1-x}\text{As}$ ($x=0.27$) 500 nm thick is grown as an inverse step to prevent the formation of MDs at the last interface. To achieve relaxation, layers have to surpass the critical thickness but, if only MDs without threading dislocations (TDs) are desired, the steps of concentration must be below the critical step concentration used by Krishnamoorthy et al. [1, 5].

The TEM observations were performed in JEOL 1200EX and 2000EX transmission electron microscopes. The cross-sectional samples were prepared by argon ion milling and the plan-view samples by chemical etching using a Br–methanol solution.

The misfit f_N of each layer is defined by the nominal lattice parameter $a_{n,N}$ of the layer of interest and by the real lattice parameter $a_{r,N-1}$ of the underneath layer. For fully strained and non-relaxed layers, $a_{n,N-1}$ and $a_{r,N-1}$ are equivalent. However, when relaxation occurs, the value of $a_{r,N-1}$ changes in relation to $a_{n,N-1}$, and $a_{r,N-1}$ is the parameter that must be considered to deduce the misfit:

$$f_N = \frac{a_{n,N} - a_{r,N-1}}{a_{r,N-1}} \quad (1)$$

InGaAs (27%)	500nm
InGaAs (30%)	125nm
InGaAs (25%)	125nm
InGaAs (20%)	125nm
InGaAs (15%)	125nm
InGaAs (10%)	125nm
InGaAs (5%)	125nm
GaAs	200nm
GaAs (100)	

Fig. 1. Schematic description of the sample structure. The steps in In concentration are 5 at.% and an inverse step is performed at the last step to obtain a non-strained layer.

The corresponding residual strain is

$$\varepsilon_N = f_N - \delta_N \quad (2)$$

where δ_N is

$$\delta_N = 1/2 p \rho_{\text{MD},N} b + (1-p) \rho_{\text{MD},N} b \quad (3)$$

$\rho_{\text{MD},N}$ is the density of MDs in the layer of interest, b is the edge dislocation Burgers vector, p is the percentage of 60° dislocations and $1-p$ is the percentage of edge dislocations. From Eqs. (1) and (2) the following general relations are deduced:

$$f_N = \sum_{i=1}^N f_i \quad (4)$$

$$\varepsilon_N = \sum_{i=1}^N (f_i - \delta_i)$$

with $f_i = \varepsilon_{i-1} + (c_i - c_{i-1})/C$, where C corresponds to the misfit of 1 at.% in In content and c_i to the In concentration of layer i .

3. Theoretical prediction of the relaxation

A few models of plastic relaxation behavior in multilayers and/or grading layers are available [8–10]. The Dunstan et al. [9, 10] geometrical model describes the relaxation in single layers, graded layers and step-graded layers. It is based on the assumption that dislocations will not form if the local induced relaxation exceeds the strain in the layer. This produces a critical thickness inversely proportional to the nominal strain ε_0 through a constant K . Passing this critical thickness, the residual strain ε_r follows a similar law, i.e. ε_r is inversely proportional to the thickness t ($\varepsilon_r/K/t$). Experimentally, K is estimated to be around 0.83 nm [9]. The extension of this model to graded layers and multilayers gives the following expression for the average strain [11]:

$$K = \int \varepsilon dt \quad (5)$$

For step-graded layers, Eq. (5) becomes

$$K = \sum_{i=0}^N \varepsilon_i t_i \quad (6)$$

Moreover, for stacks of layers, Dunstan et al. [10] propose the following relaxation process. As the $\text{In}_x\text{Ga}_{1-x}\text{As}$ begins to grow on the GaAs substrate, the growth is pseudomorphic up to the critical thickness, even if several layers of different compositions are

grown. Passing this critical thickness, dislocation loops are generated deeping to the first interface. This first process is shown in Fig. 2(a). When the first layer is totally relaxed, the growth continues pseudomorphically to this first relaxed layer. When the rest of the stack (i.e. without the first layer) passes the critical thickness loops of dislocation glide to the second interface and the second layer relaxes (Fig. 2(b)). This process continues to relax layer by layer each time that the critical thickness of the unrelaxed stack is surpassed. Finally, only a few top layers of the buffer remain strained with a total thickness $t_{tot} < \sum_i K/\epsilon_i$.

4. Results and discussion

XTEM and PVTEM observations of the step-graded sample are shown in Figs. 3(a) and 3(b) respectively. The cross-sectional transmission electron micrograph corresponds to an (004) weak-beam observation and the PVTEM corresponds to an (001) bright-field observation. The white contrasts used for the MD density determination are indicated by the arrows. Table 1 displays the MD densities measured by XTEM. The density is roughly constant for the six first interfaces. No MD is observed at the last interface. However, the MD density stays constant throughout

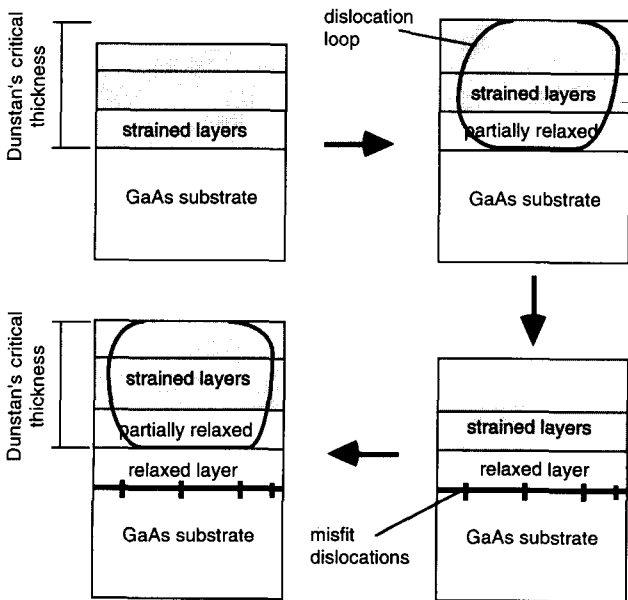


Fig. 2. Description of the relaxation in $In_xGa_{1-x}As$ multilayers grown on a GaAs substrate by Dunstan et al. [9-11] during the growth. Loops of dislocations are created during the growth when the stack of layers passes the Dunstan et al. critical thickness relaxing the first strained layer. When this first layer is relaxed, the GaAs substrate and the $In_xGa_{1-x}As$ layer behave as a single substrate and the loops relax the subsequent strained layer (the second in the figure).

This is confirmed by the PVTEM observation shown in Fig. 3(b). A density of dislocations lower than 10^5 cm^{-2} , which corresponds to the sensitivity of the method, is measured in the last step and in the cap layer is measured. No dislocations are observed along the $20 \mu\text{m}$ surrounding the hole of the TEM preparation.

From the measured MD densities at each interface and following Eqs. (1)-(4), the effective lattice parameter, the misfit, the percentage relaxation and the residual strain in each layer are deduced. Fig. 4 displays the behavior of these parameters along the whole sample structure. The difference between the nominal and the effective lattice parameters, i.e. the misfit, is shown to increase with increasing height. However, the MD density stays constant throughout

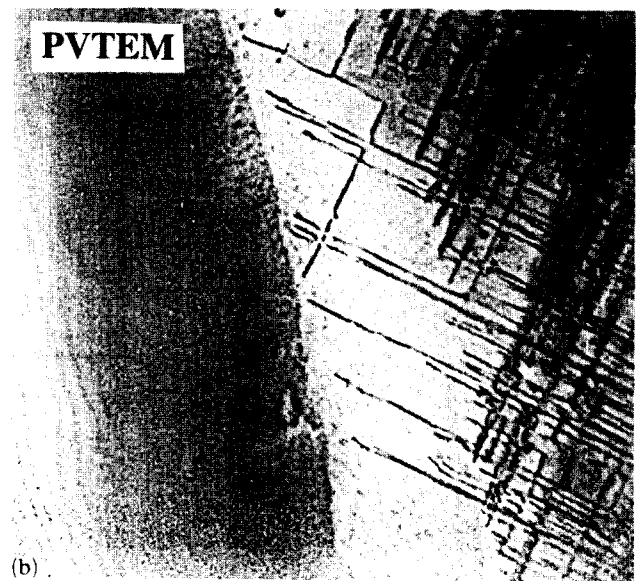
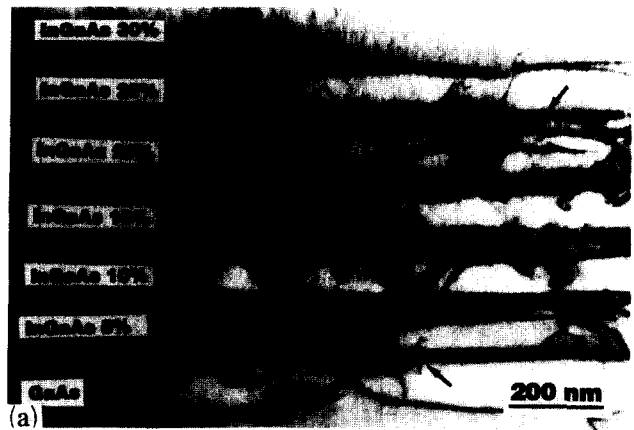


Fig. 3. (a) Cross-sectional transmission electron micrograph of the step-graded sample. (b) Planar-view transmission electron micrograph showing the low level of dislocation reaching the top surface. No contrast of the last compositional inverse step in the planar-view transmission electron micrograph is observed.

the structure. This contrasts with the behavior of single layers. In single layers, when the misfit increases, the number of MDs also increases. The percentage relaxation and the residual strain are shown to decrease and to increase respectively with increasing height. Such

behavior of the MD density is attributed to the work-hardening processes to minimize the energy state of the system due to MD interactions. The measured residual strain vs. the effective misfit for each layer of the stack is represented in Fig. 5. The behavior of the strain is

Table 1

Effective lattice parameter, effective misfit percentage relaxation and residual strain deduced from the misfit dislocation density measured by cross-sectional transmission electron microscopy

Nominal lattice parameter (at.% In content)	Effective lattice parameter (at.% In content)	Effective misfit	MD density	Relaxation (%)	Residual strain
0	0				
5	2.93	5	8.1	58.5	0.0015
10	6.78	7.06	10.6	54.4	0.0023
15	10.32	8.19	9.7	43.1	0.0033
20	14.59	9.61	11.6	4.4	0.0039
25	17.77	10.31	8.6	30.6	0.0051
30	18.51	12.08	2	6.1	0.0081
27	18.51	8.38	0	0	0.0060

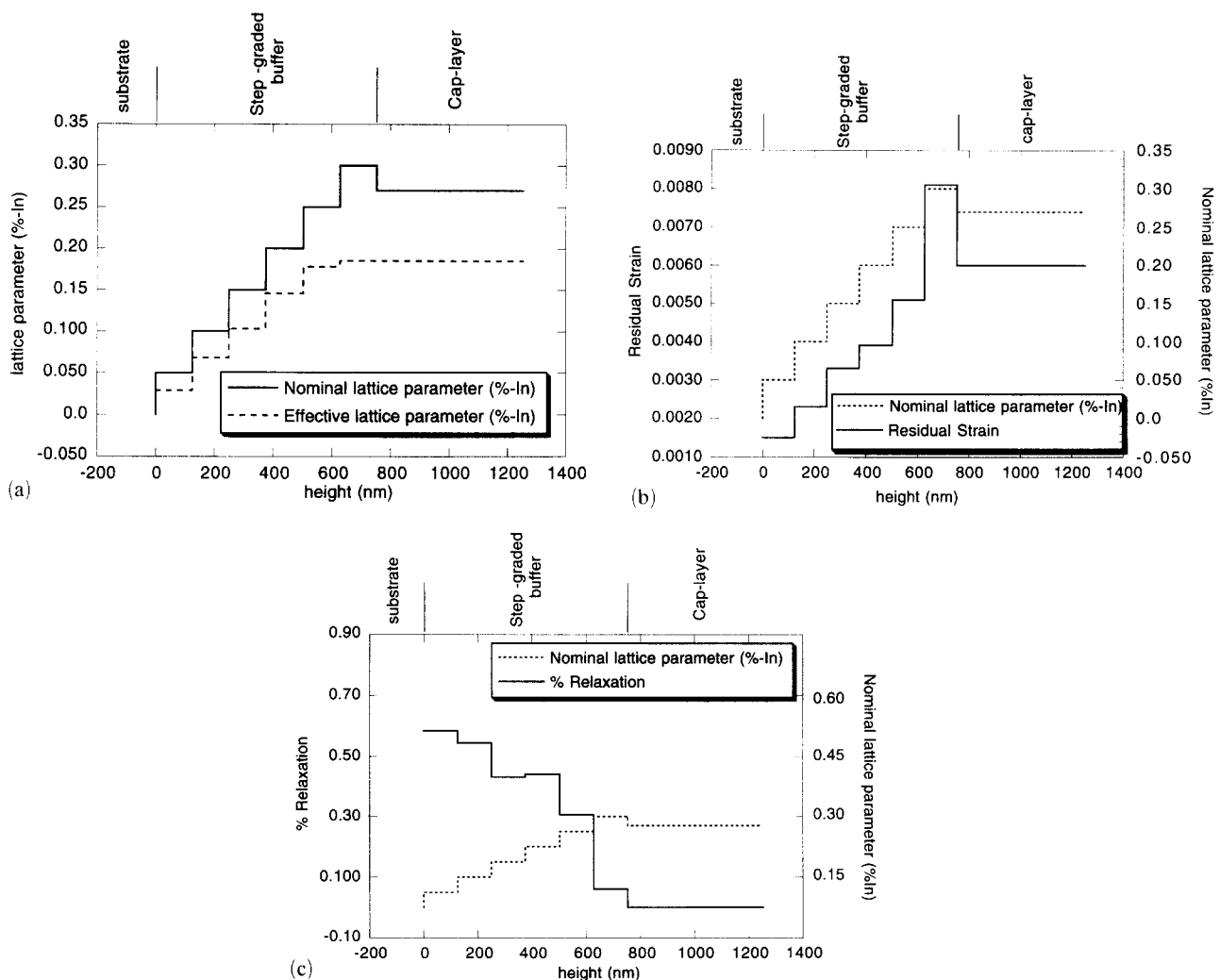


Fig. 4. (a) Real and nominal lattice parameters of the structure vs. the height. (b) Residual strain vs. the height deduced from the TEM observation. (c) Percentage relaxation vs. the height deduced from the MD density.

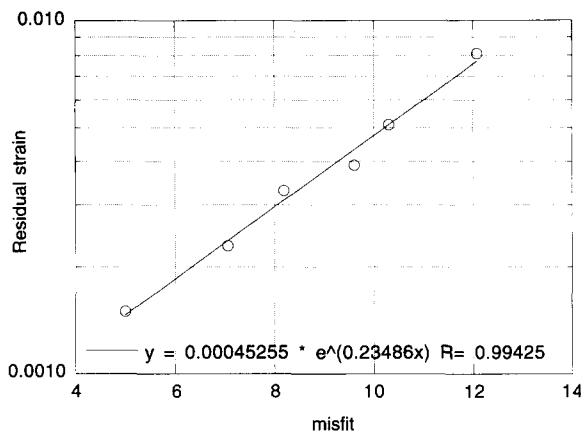


Fig. 5. Residual strain vs. the misfit. The points corresponding to the last two layers are not represented.

shown to follow an exponential behavior with the misfit. The exponential regression fits the experimental data with a correlation better than 0.99.

By applying the Dunstan et al. model to the strain results obtained (see Table 1), $K = 3.8$ nm is deduced. Moreover, as shown in Fig. 4, the relaxation behavior does not follow the Dunstan et al. model. Dislocations are observed at each interface with a nearly constant density. As the individual layer thickness is below the Dunstan et al. critical thickness ($h_c = 250$ nm), dislocations need to cross one or two interfaces to penetrate to the first interface. Interfacial effects such as the change in elastic constant can block some dislocations and then, owing to work-hardening processes, a constant distribution of MDs is reached at the equilibrium. From Eq. (4), the following recurrence expression is deduced:

$$\varepsilon_N = \varepsilon_{N-1} + f_{N,\text{nominal}} - \delta_N \quad (7)$$

Therefore work-hardening processes make δ_N constant at all the interfaces and cause ε to increase linearly with increasing thickness of the stack as confirmed by the experimental curve in Fig. 4(b). Owing to this high strain value at the top of the structure, TDs tend to bend and a dislocation-free region is observed at the top of the structure (Fig. 3(b)).

5. Conclusion

In summary, the plastic relaxation in linearly step-graded structures follows two different behaviors

depending on the individual layer thickness: (i) for layer thickness above the Dunstan et al. critical thickness, only the last layers remain strained [11]; (ii) for individual layer thicknesses below this critical thickness, work hardening induces a constant distribution of MDs at interfaces which implies, through Eq. (7), a linear behavior of the strain that increases along all the height of the structure.

Acknowledgments

This work was made possible through grants from the Comisión Interministerial de Ciencia y Tecnología (MEC), European ESPRIT Program (BLES 6854), and the Andalusian Government (Group 6020). The work was carried out at the Electron Microscopy Center of the Cádiz University. The authors wish to thank G. Aragón for many helpful discussions. P. Kidd for the X-ray measurements and J. M. Geraldía for the technical support during this study.

References

- [1] V. Krishnamoorthy, P. Ribas and R. M. Park, *Appl. Phys. Lett.*, **58** (1991) 2000.
- [2] J. C. P. Chang, Jianhui Chen, J. M. Fernandez, H. H. Wieder and K. L. Kavanagh, *Appl. Phys. Lett.*, **60** (1992) 1129.
- [3] J. C. P. Chang, T. P. Chin, C. W. Tu and K. L. Kavanagh, *Appl. Phys. Lett.*, **63** (1993) 500.
- [4] S. I. Molina, G. Gutierrez, A. Sacedón, E. Calleja and R. García, *Materials Research Society Fall Meet.*, Materials Research Society, Pittsburgh, PA, 1993.
- [5] V. Krishnamoorthy, Y. W. Lin and R. M. Park, *J. Appl. Phys.*, **72** (1992) 1752.
- [6] X. L. Wei, K. K. Fung, W. Feng and J. M. Zhon, *Appl. Phys. Lett.*, **61** (1992) 572.
- [7] D. González, D. Araújo, G. Aragón, S. I. Molina, A. Sacedón, G. Gutiérrez and R. García, *Inst. Phys. Conf. Ser.*, **138** (1993) 313.
- [8] J. Tersoff, *Appl. Phys. Lett.*, **62** (1993) 693.
- [9] D. J. Dunstan, P. Kidd, L. K. Howard and R. H. Dixon, *Appl. Phys. Lett.*, **59** (1991) 3390.
- [10] D. J. Dunstan, S. Toung and R. H. Dixon, *J. Appl. Phys.*, **70** (1991) 3038.
- [11] D. J. Dunstan, P. Kidd, P. F. Fewster, N. L. Andrew, R. Grey, J. P. R. David, L. González, Y. González, A. Sacedón and F. González, *Appl. Phys. Lett.*, in press.